Landscape Resistance Index Aiming At Functional Forest Connectivity

Ivan Vanderley-Silva (ivanvanderley@yahoo.com.br)
Federal University of São Carlos (UFSCAR-Sorocaba)
Roberta Averna Valente
Federal University of São Carlos (UFSCAR-Sorocaba)

Research Article

Keywords: Structural Equation Model, Landscape Structure Analysis, Land Use and Land Cover, and Environmental Criteria

Posted Date: June 25th, 2021

DOI: https://doi.org/10.21203/rs.3.rs-640226/v1

LANDSCAPE RESISTANCE INDEX AIMING AT FUNCTIONAL FOREST CONNECTIVITY

Ivan Vanderley-Silva, MSc[1]; Roberta Averna Valente, PhD[2]

1. Graduate Program in Planning and Use of Renewable Resources (PPGPUR), Federal University of São Carlos (UFSCAR-Sorocaba). João Leme dos Santos Highway (SP-264), km 110 – Sorocaba/SP, Brazil. ivanvanderley@yahoo.com.br. Corresponding author.

2. Environmental Sciences Department, Federal University of São Carlos (UFSCAR-Sorocaba). João Leme dos Santos Highway (SP-264), km 110 – Sorocaba/SP, Brazil. roavalen@ufscar.br.

ABSTRACT

The terrestrial surface is the basis for defining the species dispersion paths and overcoming the matrix resistance. In this approach, connecting paths with high levels of integrity must avoid barriers and anthropized areas. In this context, the main objective of this study was to develop the Landscape Resistance Index based on environment integrity. It was developed through Structural Equation Modeling (SEM), supported by the criteria of Land Surface Temperature, Nighttime Reflectance, and Inverted NDVI, which are called observed variables. The landscape studied in the Green Belt Biosphere Reserve of São Paulo has suffered from urban sprawl. However, it has significant remnants of the Atlantic Forest, which is a biodiversity hotspot. Our results indicated criteria variability in the landscape, however, modeled through the SEM, obtaining a significant adjustment of the Landscape Resistance Index, with CFI of 1.00 and RMSEA of 0.00. The index reflects the resistance levels of the land-use/land-cover, expressed by the class interval, ranging from 0% (1.73) to 100% (493.88), with the highest values associated with the anthropized uses and forest isolation. This way, the index based on environmental attributes reflects the structure of functional forest connectivity, supporting the planning design of forest corridors across landscapes.

Keywords: Structural Equation Model, Landscape Structure Analysis, Land Use and Land Cover, and Environmental Criteria.

1. INTRODUCTION

The land-use/land-cover change due to urban expansion has influenced the biodiversity, ecosystem function, and regional climate (Choudhury; Das and Das, 2018). Also, they have directly affected the surface temperature, modifying the landscape radiative, physiological, and aerodynamic properties that control the surface water and energy balances (Rigden and Li, 2017).

These environmental changes influence the occurrence, behavior, and species dispersion. Therefore, the knowledge of land-use/land-cover (LULC) influence on species dispersion is an important key for conserving the tropical forest.

In this context, Mörtberg et al. (2013) cited that the terrestrial surface is the basis to design the species dispersal path, especially when we would like to overcome the matrix resistance. Still, that the species consider the landscape as a competitive space control of the coverage. And Spear and Storfer (2010) defined the resistance of a landscape as its degree of ease or resistance to the movement of a specific species.

The resistance surfaces are developed from empirical data on gene flow, genetic distances, habitat use, movement paths (Rudnick et al., 2012) or based on expert opinion concerning focal species ability to cross landscapes (Cushman; Landguth and Flather, 2013), which has been the most used method.

This way, the researchers usually assign values to LULC, considering their resistance levels to the matter flow and energy (Feng et al., 2011), remembering that the species focal movement is random (Liu et al., 2018). However, the strong subjectivity of this method and the lack in the referential theoretical related to the human activity disturbance on the landscape (i.e., on the LULC) have been criticized (Zhang et al., 2017).

Concerning the resistance surface, Belote et al. (2016) mentioned the approach based on the connection paths with a high level of integrity, avoiding barriers and natural vegetation highly modified. The paths are the least human-modified LULC, which can linkage natural areas as protected areas and forest patches (Theobald et al., 2012).

According to Deng et al. (2018), an important factor for assessing the environment is the exchange between heat and water, which can be represented by the land surface temperature. This, considering the significant correlation between impermeable surface and temperature rise as mentioned by Silva; Silva e Santos, 2018; Rousta, et al., 2018; Niu et al., 2018; Lin et al., 2018; Du et al., 2016.

Brose et al. (2012) observed a positive correlation between the surface temperature increase and the prey-predator interaction force, as the consequence of theirs increased speeds, especially in heterothermic individuals. Also, they mentioned negative effects for species persistence in complex food webs (Brose et al., 2012), especially when there are asymmetric responses to a temperature between predators and prey (Dell; Pawar and Sawage et al., 2013).

This way, the temperature has an important role in establishing the biological organization levels standard (Gilbert et al., 2016). The metabolic ecology theory (MTE) and empirical data showed that the movement of an animal exhibits a multiple dependence between the temperature, with consequences for population dynamics and stability (Brown et al., 2004).

Therefore, it is important to know the environmental pattern where the wildlife moves because several factors contribute to surface temperature variation, especially in urban sprawl areas. Among them, there are the morphological characteristics, the heat absorption, storage, the increased heat convection (Gaur; Eichenbaun and Simonovic, 2018), the road orientation, the anthropogenic activities (Santos et al., 2017), the winds obstruction by high buildings (Zhou and Chen, 2018), the energy balance, and the hydrological cycle (Silva; Silva and Santos, 2018).

Nascimento-Júnior (2017) complemented that urban sprawl can be characterized by a socio-spatially unequal development and different degrees of environmental degradation, which can be revealed by nighttime reflectance intensity, obtained from the Linescan Operating System (LOS) of the North American Defense Meteorological Satellite Program (DMSP) (Huang et al., 2014; Chen et al., 2016; Zhang et al., 2017).

However, the dichotomous classification between urban and rural space disregards the flow of people and scenarios that connect these environments. Scenarios as the urban-rural transition composed of scattered settlements and sparsely populated areas. Others, formed by the areas that have been gradually replaced by the natural condition, having less human influence and, consequently, denser natural vegetation (Benza et al., 2016).

Throughout these scenarios, from the areas under urban sprawl to others cover by native vegetation, the LOS has registered variation on the surface temperature, following the order high-density urban area, low-density urban area, and lawn the forest. Otherwise, the traditional Normalized Difference Vegetation Index (NDVI) showed an increase in scenario values, respectively (Guha et al., 2018).

Shen et al. (2016) cited that moisture and evaporation soil reduction are the factors that decrease in temperature in agricultural areas and pasture. In forest areas, the bottom reflectance of the soil lessens the effects of the high absorption rates from short waves of the sun in the canopy, reducing the temperature (Wei et al., 2018).

In other ways, the soil reflectance in forest areas has shown fewer absorption rates than their canopy and, consequently, fewer temperature values than the agriculture and pastures (Wei et al., 2018). In forest areas, the bottom reflectance of the soil lessens the effects of the high absorption rates from short waves of the sun in the canopy, reducing the temperature (Wei et al., 2018). This way, when the focus is the forested areas, the NDVI is commonly used to identify them, as well as their biomass and potential as a habitat for communities/species as the bees (Hoagland; Beier and Lee, 2018), grasshoppers (Shi et al., 2018), birds (Bonthoux et al., 2018), and large mammals (Johnson et al., 2018; Ito et al., 2018). These studies are supported by the robust correlation between

106 plant biomass and active photosynthetic radiation absorption (Grossman, et al., 2018; Nandy, et al.,
107 2017).

108 However, Pettorelli et al. (2016) highlighted the biodiversity monitoring of the whole
109 landscape patches and not only their forested area, considering that LULC influence in vegetation
110 corridors network regional, allowing the evaluation of the pasture use intensity (Gomez-Gimenez, et
111 al., 2017), the quantification of farmland abandonment (Estel et al., 2015), and the monitoring of
112 potential protected rural areas (Weber; Schaepman-Strub and Ecker, 2018).

113 Thus, we can say that some criteria represent the landscape attributes, supporting their
114 resistance surfaces analysis for functional forest connectivity. In this context, the main objective of
115 this study was to develop the Landscape Resistance Index based on environment integrity.

116

117 **2. MATERIAL AND METHODS**

118 **2.1 Study Area**

119

120 The landscape studied (Fig. 1) is in the Green Belt Biosphere Reserve (GBBR) of São
121 Paulo (SP), which is one of the largest cities in South America (IBGE, 2021). The city has suffered
122 from the urban sprawl, resulting in pressure in its surrounding area, regarding conversion to urban
123 use to agriculture.

124 According to the United Nations United Nations Educational, Scientific, and Cultural
125 Organization (UNESCO, 2019), the Biosphere Reserve is a learning site for purposes of
126 environmental protection, logistical provision for scientific research, and educational/sustainable use
127 of natural resources. Considering the Biosphere Reserve as a place of excellence, it should support
128 ways to solve human and environmental conflicts through the local and scientific communities
129 (UNESCO, 2019).

130 The GBBR was considered of extreme importance for biodiversity conservation and to
131 design ecological corridor (MMA, 2021), considering that Atlantic Forest remnants cover 34.9% of its
132 area (165099.25 ha) belongs to Ombrophilous Dense Forestry (IBGE, 2012). Some remnants belong
133 to Protected Area as the Cabreúva Environmental Protection Area (EPA) in the North, Morro Grande
134 Forest Reserve (FR) in the South, and Itupararanga EPA in the Southwest (Fig. 1).

135 They are the most significant patches of the study area, having more than 300 ha, and
136 representing half our forest area (Table 1).

137

Table 1. Main characteristics of the forest patches of the studied landscape in the Green Belt Biosphere Reserve of São Paulo City (GBBR-SP), Brazil.

Other remnants are scattered through the matrix composed predominantly of vegetation in regeneration and unmanaged pastures (i.e., anthropic fields) and urban areas, which occupy 36.3% and 22.4% of the total study. Furthermore, in the area, there is 3.4% of planted forests (*Eucalyptus* sp), 1.4% of farmlands, 1.0% water, and 0.6% of roads (highways and rural roads), as illustrated by the LULC map (Fig.1).

We generated this map (having 90%-accuracy) through supervised classification method (Maximum Likelihood algorithm) and digitalization of anthropized areas on the screen, basing on the CBERS 4-orbital images (MUX multispectral sensor, 20 m-spatial resolution).

The anthropized areas include the low-density urban areas as well as the high-density. The first group is formed by small urban agglomerations or farms characterized by horizontal, dispersed, and polycentric growth. Thus, they were included in the analysis.

Conversely, the second group is formed by the great urban areas. They were classified as a constraint, considering their low quality for support the functional connectivity, having a compact, vertical, and monocentric shape (Ojima, 2007).

Fig. 1 - Land Use/Land Cover (LULC) and location of the study Landscape in the Green Belt Biosphere Reserve of São Paulo City (GBBR-SP), Brazil.

2.2 Conceptual Model

The Landscape Resistance Index was developed through Structural Equation Modeling, basing on the maps of Land Surface Temperature (LST), Nighttime Reflectance (Night), and Inverted NDVI (NDVIinv). These criteria represented, respectively, the physical (water and energy balance), anthropic (barriers effects), and biotics (vegetable biomass quality) attributes of the studied landscape.

The LST map was produced from a thermal infrared band of the Landsat-8, having the LULC of the studied area referential. The Night is a product of the Night and Day Bands (BND) of the Visible Infrared Imaging Radiometer Suite (VIIRS) and, the NDVIinv came from the near and infrared band of the CBERS-4.

Using a Geographic Information System, the criteria maps were sampled (7620 points randomly distributed) to support statistical analysis through the Structural Equation Modeling (SEM), where they were our observed variables.

This way, modeling these variables, we obtained the Landscape Resistance Index, which was our latent variable in the SEM context (Fig. 2).

2.3 Structural Equation Modeling (SEM)

The Structural Equation Modeling (SEM) is a multivariate technique used to analyze a group of observed variables, following a holistic hypothesis previously established and having the ability to represents non-measurable variables, named latent variables or constructs (Grace et al., 2010).

As we mentioned, the observed variables were the maps of LST, Night, and NDVIinv to indicate the way related with the least resistance in the landscape, basing on the ecology integrity concept.

This way, the Landscape Resistance Index (LRI) constitutes the latent variable (dependent variable), which is a theorized and unobserved concept measured indirectly by the consistency analysis among multiple observed variables (independent variable). These indicators represent the theoretical concept response, and they include measurement error explanation (Hair et al. 2009).

Remembering that SEM is based on Leopold's model (1949). So, it refers to ecosystem integrity that has not undergone an anthropic change. Nowadays, it is understood as a holistic and structural concept, focusing on natural variations to promote conservation of native biodiversity (Keenleyside, 2012). Thus, the ecological systems that retain their native species and natural processes are, hypothetically, the most resistant and resilient to anthropogenic and natural stress (Woodley, 2010).

According to Grace et al. (2010), the SEM also involves multiple regression problems using a path diagram. The unidirectional arrow indicates the cause-effect relationship between the variables, and the double arrows indicate the covariances relationship.

In general, the steps for building the model were the theoretical basis, model elaboration, collection and preparation of variables, estimation, adjustment assessment, and discussion (Kaplan, 2000).

Fig.2 - Conceptual model used to obtain the Landscape Resistance Index for the Green Belt Biosphere Reserve of São Paulo City (GBBR-SP), Brazil**.**

2.4 Observed Variables

The criteria definition to support our index development considered that the animal movement across the landscape is a complex process involving the local environment's characteristics (Hooten et al., 2010). Furthermore, the indication of Hanks, Hooten, and Alldredge (2015) and Wilson, Hanks, and Johnson (2019) that the barriers to animal movement and their preferred habitat as environmental covariables assess animal behaviors.

This way, Table 2 shows the main reason for modeling the LST, Night, and NDVIinv to obtain the Landscape Resistance Index.

Table 2. LST, NDVIinv, and Night: brief justifies to modeling the landscape resistance, aiming at functional forest connectivity in the landscapes under urban sprawl.

The satellite images supported the observed variables production. LST used the thermal infrared, band 10 of the Landsat-8 (TIRS sensor), to determine our LULC terrestrial surface temperature. However, its original 100 m-spatial resolution was resampled to 20m, which is the same as the LULC map.

The band atmospheric correction followed the available parameters on the United States Geological Survey website (USGS, 2019). This way, the later radiance value was converted to Kelvin temperature and after to degrees Celsius (ºC), subtracting 273,15 K (Barsi; Barker and Schott, 2003). In this sense, the LST map represents the areas where the energy and water balance were the most intense of the landscape, therefore, the most unfavorable to the gene flow.

The Night map constituted in the Night and Day Band (BND) of the Visible Infrared Imaging Radiometer Suite (VIIRS), which was provided by the Earth Observation Group (EOG) of the National Center for Environmental Information (NCEI). In the literature, the Night is considered effective in determining urban areas (Su, et al., 2015; Zhou et al., 2014), in this study, to identify anthropic barriers to gene flow. In the same way, its 450 m-spatial resolution was standardized to 20m. However, the available images were firstly filtered to exclude data affected by diffuse light, lightning, lunar illumination, and cloud cover addition, and border bands were excluded, the called aggregation zones.

The NDVI was generated from CBERS-4 satellite images (MUX sensor, 20m- spatial resolution). The index is traditionally used to analyze vegetation vigor, considering that energy reflected in the red and near-infrared regions is inversely related. The result is directly proportional

to the green biomass, represented by values closer to +1, indicating vegetation denser, moist, and well-developed (Gitelson; Peng and Huemmrich, 2014).

In this context, we multiplied NDVI by -1m, using a raster calculator, to obtain NDVIinv, considering that values near -1 represent LULC with the most resistance to flow gene since they have less vegetable biomass.

The LST, NDVIinv, and Night maps were normalized to a common scale, ranging from 0 to 255, using linear function. After, they were sampled considering 7620 points randomly distributed through the study area, having a minimum distance among them of 100m. This sample size corresponds to 20 times the statistical sampling required for a 95% confidence interval and 5% error.

2.5 Landscape Resistance Index

The Structural Equation Model used to obtain the LRI is described in eq. 1, which was normalized for 0 to 100% as indicated eq.2.

Eq. 1. Structural Equation Model used to obtain the Landscape Resistance Index (LRI) for the study landscape in the Green Belt Biosphere Reserve of São Paulo City (GBBR-SP), Brazil.

$$\mathbf{LRI} = (((\mathbf{Factor\ LST} * \mathbf{LST}) + \mathbf{Error\ LST}) + (\mathbf{Factor\ NDVIinv} * \mathbf{NDVIinv}) + \mathbf{Error\ NDVIinv})) + ((\mathbf{Factor\ Night} * \mathbf{NIght}) + \mathbf{Error\ Night}))).$$

Eq. 2. Landscape Resistance Index (LRI) normalized for percentage for the study landscape in the Green Belt Biosphere Reserve of São Paulo City (GBBR-SP), Brazil.

$$\mathbf{LRI}\% = (\left(\frac{\mathbf{100}}{\mathbf{Max\ LRI} - \mathbf{Min\ LRI}}\right) * (\mathbf{LRI} - \mathbf{Max\ LRI})) + \mathbf{100}$$

Where: Factor and error are indicators obtained in the Structural Equation Model for each environmental attributes; Max = Value Maximum; Min = Value Minimum.

Using the Semplot package (R program), we estimated the factors and errors considering data previously tested to correlation and normal distribution.

The Comparative Fit Index was used to fit test, in the context of the model complexity analysis (Byrne, 2009), and the Root Mean Square Error of Approximation (RMSEA) to assess how well the model fits a population and not just a sample estimated (Hair et al., 2009), as discussed in the specialized literature (Ullman, 2006).

For model adjustment, values greater than 0.90 for CFI and less than 0.10 for RMSEA were adopted as parameters proposed by Gama-Rodrigues (2014). In addition, the factor parameter must be statistically significant. According to Hair et al. (2009), an appropriate value must be greater than 0.50, being ideals greater than 0.70. Also, according to the authors, a Construct Reliability (CR) is a good convergent validity indicator. Values between 0.6 and 0.7 may be acceptable if other indicators are good. But, for all measures to represent the construct, CR must be greater than 0.70.

2.6 Index spatialization

The LRI% spatialized in the GIS supported different analyses. Firstly, on a continuous scale (%), we evaluated three scenarios, that were its distribution (i) through our studied area, (ii) without the forest patches, and (iii) only inside these forest patches.

After, the studied area was classified in the level of resistance very low, low, medium, high, and very high, though the Jenk Natural Break method, an algorithm that maximizes similarity within classes and the distance between groups (Smith; Goodchild and Longley, 2018). And we analyzed the overlap between resistance and LULC classes.

Finally, we analyzed the relation between resistance and functional forest connectivity, considering the forest patches as the reference.

So, we generated the Euclidean distance from the forest patches centroids, which was evaluated together with the resistance classes map, using a sample of 7620 points.

In the statistic program, the distance data were log (x+1) transformed and applied the Generalized Linear Model of binomial regression for each resistance class. For this, it was considered the presence (1) or absence (0) of the resistance class (dependent variable) depending on Euclidean distance from forest fragments centroids (independent variable).

2 RESULTS

The environmental attributes (in 255 bytes) that supported the LRI modeling for the Green Belt Biosphere Reserve (SP, Brazil) are in Fig. 3.

The predominant values of NDVI and Night were represented by at most 50 bytes, which occupied 73% of our studied area on the first map and 93% on the second. The medium value on the NDVI map was 34.8 bytes (DV: ± 52.8), whereas the Night map was 12.1 bytes (± 39.8).

The LST was the variable with the greatest variability in the landscape, having 92.1% of our total area associated with values lower than 150 bytes (medium value: 68.8 e ± 63.7).

These attributes, i.e., observed variables in the model context, contributed to a significant adjustment of the Landscape Resistance Index (IRP), with CFI of 1.00 and RMSEA of 0.00 (Fig. 4A).

This way, the factor loading obtained for the LST, Night and NDVIinv was respectively of 0.56 (error = 0.68), 0.57 (error = 0.68), and 0.80 (error = 0.37). Highlighting the significant adjustment that we obtained on the standardized assessment among these factor loads (calculated by the model) and on the sum of the points representing them.

The Construct Reliability (CR) of the model was 0.68, that is, considered adequate, even presenting a great data variation in the intermediate values (between 400 and 800 points)

Fig. 3. Environmental attributes (in 255 bytes) for the study area in the GBBR-SP, Brazil: (A) Inverted NDVI, (B) Land Surface Temperature, and (C) Nighttime Reflectance.

Fig.4 – Landscape Resistance Index for the study area in the GBBR-SP, Brazil: (A) parameters and factor loadings modeled, and (B) model CR, based on the sum of the points representing the OV and their factor loadings.

In this context, the SEM used to obtain the LRI is presented in eq.3:

Eq. 3. Landscape Resistance Index (LRI) for the study landscape in the Green Belt Biosphere Reserve of São Paulo City (GBBR-SP), Brazil.

$$\mathbf{LRI} = (((\mathbf{0.80} * \mathbf{NDVIinv}) + \mathbf{0.37}) + (\mathbf{0.57} * \mathbf{NIGHT}) + \mathbf{0.68}) + ((\mathbf{0.56} * \mathbf{LST}) + \mathbf{0.68}))$$

Where: Inverted NDVI (NDVIinv), Nighttime Reflectance (Night), Land Surface Temperature (LST), and Landscape Resistance Index (LRI).

The model (eq. 3) resulted in an LRI ranging from 1.73 to 493.88 for our study area, justly reflecting the internal disparities of the matrix components in terms of resistance to genetic flow. These LRI threshold values are in the eq.4 to normalize LRI from 0-100% (Fig. 5).

Eq. 4. Landscape Resistance Index (LRI) normalized for percentage for the study landscape in the Green Belt Biosphere Reserve of São Paulo City (GBBR-SP), Brazil.

$$\mathbf{LRI\%} = (\left(\frac{\mathbf{100}}{\mathbf{492.15}}\right) * (\mathbf{LRI} - \mathbf{493.88})) + \mathbf{100}$$

Where: Landscape Resistance Index (LRI) and, and Landscape Resistance Index normalized for percentage (LRI%).

Fig. 5 - LRI% spatialized through the studied area (Fig. 5A), without the forest patches (Fig. 5B), and only inside these patches (Fig. 5C).

This way, the resistance inside the forest patches is small than the matrix, although with different levels, as we also observed for the matrix components (urban areas, planted forest, farmlands, water, road, and anthropized fields).

Remembering that the urban areas refers to small urban agglomerations (low-density urban area) and great urban areas (high-density urban area), while anthropized fields are predominantly composed by vegetation in regeneration and unmanaged pastures.

Evaluating our study area in classes of resistance (Table 3), we obtained 36.3% of its total area classified as very low, 31.5% as low, 20.4% as a medium, 8.2% as high, and 3.6% as very high. Still, a special association of them with the native forest, high density urban area, and anthropized field.

The native forest occupied 76% of the very low class, 23% of the low, and less than 2% of other classes. Otherwise, anthropized fields predominated in the low and medium classes, representing 55% and 62% of them. It also was the second use, with 36%, in the high class.

The most resistant land use of our landscape, represented by the high-density urban area, prevailed in the very high and high classes, occupying 92% and 51% of their respective total areas.

Table 3 also indicated the presence of planted forest in 7% of the very low class, in 3% of the low class, but it is associated with or close to native forest or abandoned anthropized fields.

Table 3 – The LULC and resistance classes of the study area, located in GBBR-SP, Brazil.

Relating the analysis of resistance and functional forest connectivity, our results indicated coherence between the occurrence of resistance classes and the forest patches distance from their respective centroid (Fig.6).

Fig.6 - Binomial regression Generalized Linear Model (GLM) for LRI resistance classes, depending on forest patches distance from their centroids of the studied landscape, in the GBBR-SP, Brazil.

The frequency of high and very high resistance classes increased with the distancing from the patches centroids (Fig. 6D/E). While, the very low and medium class frequencies decreased (Fig. 6 B/C). Unlinked, very low resistance increased with the distancing from the patches centroids, reflecting the presence of the large forest patches in the studied area (Fig. 6A). Especially, those having more than 300 ha (Table 1), where there is a great distance between their centroid and edge, traversing great distances within the forest fragments.

3 DISCUSSION

The landscape studied in the Green Belt Biosphere Reserve of São Paulo supported the modeling of the Landscape Resistance Index (Fig. 4A, CFI of 1.00 and RMSEA of 0.00).

In turn, the index reflects the resistance levels of the land-use/land-cover, expressed by the class interval, ranging from 0% (1.73) to 100% (493.88), with the highest values associated with the anthropized uses and forest isolation (Table 3. Fig. 6). This way, LRI supports the design of forest corridors through environmental with the lowest resistance.

The criteria (i.e., observed variables) supported the LRI modeling, considering their variability and importance to functional forest connectivity.

NDVIinv showed 73% (± 52.8) of the landscape below 50 bytes, representing the highest forest density environments. Consistently, in that same byte portion, Night presented 93% (± 39.8) of the landscape, that is, environments with less influence from urbanized areas. And, LST 92.1% (± 63.7) of occurrences below 150 bytes and, therefore, greater distribution and variation in the landscape (Fig. 3).

This way, our criteria represented the landscape attributes as the LULC, topography, and indicators of anthropogenic disturbance (Wasserman, et al., 2010, Neumann et al., 2015, Mateo-sánchez et al., 2015, Krishnamurthy et al., 2016, Milanesi et al., 2017). This representativeness is important since they influence the resistance, which in turn is related to habitat adequation. Still, when we remember that while the landscape resistance is related to a point surface value, the connectivity is cumulative to movement across the dispersal surface (Cushman, Lewis, and Landguth, 2014, Krishnamurthy et al., 2016). Thus, spatial correlations are fundamental to infer the dispersion capacity of species in the environment (Bajaru et al., 2020).

According to our results, the NDVIlin represents the association between animal behavior and landscape structure described for different animal species (Fig. 3A). Some studies have shown that animals moving in the landscape respond to environmental changes, especially influenced by vegetation (Remegaldo, Safi, Wegmann, 2019, Da Silveira, 2016, Brown, et al., 2017), which can identify through the vegetation indexes (Pettorelli et al., 2011).

In the same way, our criteria LST represents the temperature effects on the ecological processes (Fig. 3B). According to Delong (2012), temperature influences the animal movement across the landscape, and its variation influences the quality of the movement (Pawar et al., 2016, Gilbert et al., 2016).

Robinson et al. (2013) remembered that the species persistence depends on the ability of the specimens to tolerate thermal changes in the landscape and on the thermal suitability of the

habitat, which varies spatially according to the soil cover and surrounding vegetation (Robinson et al., 2013). Consequently, gradients thermal effects affect habitat selection (Nowakowski et al., 2016).

Our last criterion was the Night, representing the artificial light irradiated by the anthropized environment, i.e., our artificial barriers to gene flow and light disturbances (Fig. 3C). Resulting from urban sprawl, this light pollution gradually invades natural environments and generates greater resistance to photosensitive species in habitats close to impact sources (Guetté, et al., 2018, Davies e Smyths, 2018, Gaston e Holt, 2018).

Considering their high variability, the criteria influenced differently on LRI with NDVIinv showing the highest factor loading (n) and lowest error (error) among the three. Their values were 0.80 and 0.37, whereas LST and Night showed n of 0.56 and an error of 0.68 (Fig. 4A).

Therefore, the model assumes that the greatest resistance is correlated with the sum of the criteria factor loads (Eq. 3 e 4). Consequently, with the regions with the highest plant biomass, the lowest temperature on the Earth surface, and the lowest presence of anthropized areas.

However, there was a greater dispersion of results in environments of moderate resistance, that is, those in transition between forests and urban areas (Fig. 4B).

As a positive point of the index is it reflects the resistance levels of the land-use/land-cover, expressed by the class interval, ranging from 0% (1.73) to 100% (493.88), with the highest values associated with the anthropized uses and forest isolation (Eq. 3 e 4).

The model predictability for our landscape is 88%, having the most variability in the matrix (Fig. 5), which is formed by environments with high values of resistance (88%) as well as low (0%). Thus, even in anthropized areas, the index supports the identification of micro-habitats, identified by where the animals move and by behavioral pattern (Peterman et al., 2014, Reding et al., 2013, Zeller et al., 2012).

The predictability for forest fragments, which was 53%, shows this characteristic of reflecting heterogeneity inserted in the model through the criteria (Fig. 5C and Table 3). So, using the index, we can identify places where species can occupy or move in these environments, conferring characteristics of resilience or ecological resistance to the spatialization of landscape resistance (Nimmo et al., 2015, Robinson et al., 2013).

In the same way, when we classified the landscape in classes of the index, we obtained the very low resistance environments associated with forest fragments (75.9%) while very high resistance regions with urban areas (91.9%). In the intermediate environments, there was a transition process from the natural to the urbanized LULC due to the increase in resistance, especially for anthropized fields, planted forests, and agriculture (Table 3).

In this sense, the reports that the landscape structure is only one component of the many affecting functional connectivities and that individuals can traverse inadequate habitats during dispersal corroborate the stratified analysis of the IRP (Baguette et al., 2013, Froidevaux et al., 2016, Melin et al., 2016). Thus, the resistance of the landscape can vary according to the dispersion capacity of the species (Liu et al., 2018) and the sensitivity to barriers (Breckheimer et al., 2014).

This coexistence structure between animals and anthropized environments is reported in the literature with carnivores, small mammals, and multi-species (König et al., 2020, Chapron et al., 2014, Ceia-Hasse et al., 2017, Loveridge et al. 2017, Ducci et al., 2015, Bajaru et al. 2020). In this perspective of heterogeneity of resistance in the landscape, the analysis of the IRP performance showed coherence and the increase of forest isolation (Fig. 6).

In this context, as the consequence of the great forest patches (area) in the landscape (Table 1), we obtained the increase in very low resistance environments due to the greater distance from the centroid of forest fragments (Fig. 6A). Although the resistance to movement in these great patches is meager, so we cannot affirm that the functional connectivity promotes the structuring of the local community in these regions (Poniatowski et al., 2016, Lindenmayer et al., 2020).

Otherwise, our findings indicate that the increase in the distance from the forest patches is proportional to the occurrence of regions with very high and high resistance (Fig. 6D/E), as urban areas and highways in these environments, the low capacity for connectivity performs a species filtering, mediated by habitat characteristics, which will result in an unequal probability of species occurrence (Salgueiro et al., 2021, Kurz et al., 2014). Associating with the low and medium resistance environments, we observe the predominance of anthropized fields in different stages of regeneration and planted forests and agriculture. Remarking that they are near forest fragments was one of the decisive factors for defining their resistance and occurrence. Chazdon and Uriarte (2016) also observed places close to forest fragments, reporting rapid natural regeneration.

According to Dallabrida et al. (2019), the dynamics of the bush-tree component is not a spatially homogeneous process, having factors ecological, biotic, and abiotic influencing the demographic rates of the regenerative component and which will affect biodiversity conservation (Salami et al., 2014, Arroyo-Rodriguez et al., 2017).

In this approach, in intermediate resistance environments, sensory perception plays an important role for the animal during movement across the landscape (Clarke, et al. 2013). Remembering that the animals need the acquisition, interpretation, selection, and organization of sensory impressions to assign meaning to the surrounding environment, based on their respective life history and, for some animals depending on their memory (Almeida et al., 2010).

4 CONCLUSION

The study was developed for landscapes, as our studied area, that has suffered from urban sprawl, although that have significant remnants of the Atlantic Forest, which is a biodiversity hotspot. Remnants that support ecological processes and species dispersion across the environment.

In this scenario, our challenge was identifying the paths basing on the LULC resistance, aiming at the forest functional connectivity. Even more, considering landscape attributes instead of a species dispersion pattern. Attributes that could be modeled to obtain the Landscape Resistance Index. In this study, they were modeled through the Structural Equation Model, naming observed variables.

Thus, our observed variables are NDVIinv, Night, and LST, which are robust to determine the landscape resistance, aiming at functional forest connectivity. They have different influences on the landscape and, consequently, on the index, resulting in spatial heterogeneity associated with the movement across the landscape.

This way, LRI supports the definition of limits minimum (1.73 = 0%) and maximum (493.88 = 100%), reflecting LULC with different resistance. Its spatialization indicates regions of very low resistance associated with forest fragments, of very high with urban areas, and regions with intermediate levels having a transition process from the natural to the urbanized LULC due to the increase in resistance, especially for anthropized fields, planted forests, and agriculture.

Finally, we conclude that the index based on environmental attributes reflects the structure of functional forest connectivity, supporting the planning design of forest corridors across landscapes.

ACKNOWLEDGMENTS

The authors would also like to acknowledge the Federal University of São Carlos (UFSCAR-Sorocaba) for the opportunity to carry out this study.

DECLARATIONS

Funding

This work was supported by the São Paulo Research Foundation – FAPESP (process number 2018/21612-8).

Conflicts of interest/Competing interests

The authors declare that they have no known competing financial interests or personal relationships that could have appeared to influence the work reported in this paper.

Availability of data and material

Data and materials may be made available.

Code availability

Not applicable

Authors' contributions

Not applicable

Ethics approval

Not applicable

Consent to participate

Not applicable

Consent for publication

Not applicable

REFERENCES

Abrahms, B., S. C. Sawyer, N. R. Jordan, J. W. McNutt, A. M. Wilson, and Brashares, J. S., 2017. Does wildlife resource selection accurately inform corridor conservation? J. Appl. Ecol. 54:412–422. https://doi.org/10.1111/1365-2664.12714

Alagador, D., Triviño, M., Cerdeira, J.O. et al. 2012. Linking like with like: optimising connectivity between environmentally-similar habitats. Landscape Ecology. 27: 291–301. https://doi.org/10.1007/s10980-012-9704-9

Almeida, M., Almeida, A., Almeida, M., 2010. Reeducação psiconeurológica. 1ª Ed. Biblioteca 24 horas. São Paulo. ISBN 978857893-535-1.

Alston, J. M., Joyce, J. M., Merkle, J. A., et al., 2020. Temperature shapes movement and habitat selection by a heat-sensitive ungulate. Landscape Ecology. 35:1961–1973. https://doi.org/10.1007/s10980-020-01072-y.

Arroyo-Rodríguez, V., Melo, F., Martinez-Ramos, M., Bongers, F., et al., 2017. Multiple successional pathways in human-modified tropical landscapes: New insights from forest succession, forest fragmentation and landscape ecology research. Biological Reviews, 92(1):326–340. https://doi.org/10.1111/brv.12231

526 Baguette, M., et al. 2013. Individual dispersal, landscape connectivity and ecological networks.
527 Biological Reviews 88: 310–326. https://doi.org/10.1111/brv.12000.

528 Bailey, J., Wallis, J., & Codling, E., 2018. Navigational efficiency in a biased and correlated random
529 walk model of individual animal movement. Ecology, 99(1):217-223. Retrieved June 1,
530 2021, from https://www.jstor.org/stable/26624027.

531 Bajaru, S., Pal, S., Prabhu, M., et al., 2020. A multi-species occupancy modeling approach to
532 access the impacts of land use and land cover on terrestrial vertebrates in the Mumbai
533 Metropolitan Region (MMR), Western Ghats, India. Plos One. 15(10): e0240989.
534 https://doi.org/10.1371/journal.pone.0240989.

535 Barsi, J., Barker, J. L., Schott, J. R., 2003. An Atmospheric Correction Parameter Calculator for a
536 Single Thermal Band Earth-Sensing Instrument. " IGARSS 2003. 2003 IEEE International
537 Geoscience and Remote Sensing Symposium. Proceedings (IEEE Cat. No.03CH37477),
538 Toulouse, 5:3014-3016. https://doi:10.1109/IGARSS.2003.1294665.

539 Belote, R. T., Dietz, M. S., McRae, B. H., et al., 2016. Theobald DM, McClure ML, Irwin GH, et
540 al. Identifying corridors among large protected areas in the United States. PLoS ONE. 11(4)
541 https://doi.org/10.1371/journal.pone.0154223.

542 Benza, M., Weeks, J. R., Stow, D. A., López-Carr, D., Clarke, K. C., 2016. A pattern-based definition
543 of urban context using remote sensing and GIS. Remote Sensing of Environment. 183:250-
544 264. https://doi.org/10.1016/j.rse.2016.06.011.

545 Berger-Tal, O., Saltz, D., 2019. Invisible barriers: anthropogenic impacts on inter- and intra-specific
546 interactions as drivers of landscape-independent fragmentation. Philos Trans R Soc Lond
547 B Biol Sci.. 374(1781):20180049. https://doi.org/ 10.1098/rstb.2018.0049.

548 Bonthoux, S., Lefèvre, S., Herrault, P. A., Sheeren, D., 2018. Spatial and Temporal Dependency of
549 NDVI Satellite Imagery in Predicting Bird Diversity over France. Remote
550 Sens. 10(7):1136. https://doi.org/10.3390/rs10071136.

551 Breckheimer, I., Haddad, N., Morris, W., Trainor, A., et al., 2014. Defining and evaluating the
552 umbrella species concept for conserving and restoring landscape connectivity.
553 Conservation Biology 28:1584–1593. https://doi.org/10.1111/cobi.12362

554 Broders, H. G., Coombs, A.B., McCarron, J. R., 2012. Ecothermic responses of moose (Alces alces)
555 to thermoregulatory stress on mainland Nova Scotia. Alces 48:53–61.

556 Brose, U., Dunne, J. A., Montoya, J. M., et al., 2012. Climate change in size-structured ecosystems.
557 Phil. Trans. of the Royal Society B. 367:2903-2912. http://doi.org/10.1098/rstb.2012.0232.

558 Brown, J. H., Gillooly, J. F., Allen, A. P., et al., 2004. Toward a Metabolic Theory of Ecology. Ecology
559 Society of America. 85(7):1771-1789. https://doi.org/10.1890/03-9000.

560 Brown, L. M., Fuda, R. K., Schtickzelle, N., et al., 2017. Using animal movement behavior to
561 categorize land cover and predict consequences for connectivity and patch residence
562 times. Landscape Ecology. 32:1657–1670. https://doi.org/10.1007/s10980-017-0533-8.

563 Brown, L. M., R. K. Fuda, N. Schtickzelle, H. Coffman, A. Jost, A. Kazberouk, et al. 2017. Using
564 animal movement behavior to categorize land cover and predict consequences for
565 connectivity and patch residence times. Landscape Ecol. 32:1657–1670.
566 https://doi.org/10.1007/s10980-017-0533-8.

567 Byrne, B. M., 2009. Structural equation modeling with AMOS: basic concepts, applications and
568 programming, 2ª edition. Routledge.

569 Ceia-Hasse, A., Borda-de-água, L., Grilo, C., et al., 2017. Global exposure of carnivores to roads.
570 Global Ecology and Biogeography. 26(5):592-600. https://doi.org/10.1111/geb.12564.

571 Chapron G., Kaczensky, P., Linnell, J. D. C., et al., 2014. Recovery of large carnivores in Europe's
572 modern human-dominated landscapes. Science 346:1517 – 1519.
573 https://doi.org/10.1126/science.1257553.

574 Chazdon, R. L., Uriarte, M., 2016. Natural regeneration in the context of large-scale forest and
575 landscape restoration in the tropics. Biotropical. 48(6):709-
576 715. https://doi.org/10.1111/btp.12409

577 Chen, Y., Li, X., Liu, X., Ai, B., Li., S., 2016. Capturing the varying effects of driving forces over time
578 for the simulation of urban growth by using survival analysis and cellular
579 automata, Landscape Urban Planning, 152:59-71.
580 https://doi.org/10.1016/j.landurbplan.2016.03.011.

581 Choudhury, D.; Das, K.; Das, A., 2018. Assessment of land use land cover changes and its impact
582 on variations of land surface temperature in Asansol-Durgapur Development Region. The
583 Egyptian Journal of Remote Sensing and Space Science. 22(2):203-218. https://doi.org/
584 10.1016/j.ejrs.2018.05.004.

585 Clarke, A., Taylor, K. I., Devereux, B. et al., 2013. From Perception to Conception: How meaningful
586 objects are processed over time, Cerebral Cortex, 23(1);187–
587 197. https://doi.org/10.1093/cercor/bhs002.

588 Cushman, S. A., Landguth, E. L., Flather, C. H., 2013. Evaluating population connectivity for
589 species of conservation concern in the American Great Plains. Biodivers Conserv 22: 2583–
590 2605. https://doi.org/10.1007/s10531-013-0541-1.

591 Cushman, S. A., Lewis, J. S., Landguth, E. L., 2014. Why Did the Bear Cross the Road? Comparing
592 the Performance of Multiple Resistance Surfaces and Connectivity Modeling Methods.
593 Diversity. 6(4):844-854. https://doi.org/10.3390/d6040844

594 Da Silveira, N. S., B. B. S. Niebuhr, R. de Lara Muylaert, M. C. Ribeiro, and M. A.
595 Pizo. 2016. Effects of land cover on the movement of frugivorous birds in a heterogeneous
596 landscape. PLoS ONE. 11:e0156688. https://doi.org/ 10.1371/journal.pone.0156688.

597 Dallabrida, J. P., Silva, A. C., Higuchi, P. L., et al., 2019. Expansão da vegetação arbustivo-arbórea
598 em áreas abertas alto-montanas adjacentes a fragmentos florestais, no Planalto Sul
599 Catarinense. Ciência Florestal, 29(1):130-143.https://doi.org/10.5902/1980509825998.

600 Davies, T. W., Smyth, T., 2018. Why artificial light at night should be a focus for global change
601 research in the 21st century. Global Change Biology. 24:872–882.
602 https://doi.org/10.1111/gcb.13927.

603 de Castro, A., J. Six, R. Plant, and J. Peña. 2018. Mapping crop calendar events and phenology-
604 related metrics at the parcel level by Object-Based Image Analysis (OBIA) of MODIS-NDVI
605 time-series: a Case Study in Central California. Remote Sens. 10:1745.
606 https://doi.org/10.3390/rs10111745.

607 Dell. A. I., Pawar, S., Savage, V. M., 2013. Temperature dependence of trophic interactions are
608 driven by asymmetry of species responses and foraging strategy. Journal of Animal
609 Ecology. 83(1):70-84. https://doi.org/10.1111/1365-2656.12081.

610 DeLong JP. 2012. Experimental demonstration of a ‘rate-size’ trade-off governing body size
611 optimization. Evolutionary Ecology Research 14:343-352.

612 Deng, Y., Wang, S., Bai, X. et al., 2018. Relationship among land surface temperature and LUCC,
613 NDVI in typical karst area. Sci Rep 8(641). https://doi.org/10.1038/s41598-017-19088-x.

614 Dong, J., X. Xiao, M. A. Menarguez, G. Zhang, Y. Qin, D. Thau, et al. 2016. Mapping paddy rice
615 planting area in northeastern Asia with Landsat 8 images, phenology-based algorithm and

Google Earth Engine. Remote Sens. Environ. 185:142–154. https://doi.org/10.1016/j.rse.2016.02.016.

Du, H., Wang, D., Wang, Y., et al., 2016. Influences of land cover types, meteorological conditions, anthropogenic heat and urban area on surface urban heat island in the Yangtze River Delta Urban Agglomeration. Science of the Total Environmental. 571:461-470. https://doi.org/10.1016/j.scitotenv.2016.07.012.

Ducci, L., Agnelli, P., Di Febbraro, M., et al., 2015. Different bat guilds perceive their habitat in different ways: a multiscale landscape approach for variable selection in species distribution modelling. Landscape Ecology. 30:2147-2159. https://doi.org/10.1007/s10980-015-0237-x

Estel, S., Kuemmerle, T., Concepcion, P. C. A., Levers, C. et al., 2015. Mapping farmland abandonment and recultivation across Europe using MODIS NDVI time series. Remote Sensing Environmental. 163:312–325. https://doi.org/10.1016/j.rse.2015.03.028.

Feng, Y., Luo, G., Lu, L. et al. 2011. Effects of land use change on landscape pattern of the Manas River watershed in Xinjiang, China. Environ Earth Sci. 64:2067–2077. https://doi.org/10.1007/s12665-011-1029-5.

Froidevaux, J. S. P., F. Zellweger, K. Bollmann, G. Jones, and M. K. Obrist. 2016. From field surveys to LiDAR: shining a light on how bats respond to forest structure. Remote Sensing of Environment 175:242–250.https://doi.org/10.1016 / j.rse.2015.12.038.

Gama-Rodrigues, A. C., Sales, M. V. S., Silva, P. S. D., et al., 2014. An exploratory analysis of phosphorus transformations in tropical soils using structural equation modeling. Biogeochemistry. 118:453–469. https://doi.org/10.1007/s10533-013-9946-x.

Gaston, K. J., Holt, L. A., 2018. Nature, extent and ecological implications of night-time light from road vehicles. The Journal of Applied Ecology. 55:2296–2307. https://doi.org/10.1111/1365-2664.13157.

Gaur A., Eichenbaum M.K., Simonovic S.P., 2018. Analysis and modelling of surface Urban Heat Island in 20 Canadian cities under climate and land-cover change. J Environ Manage. 206:145-157. https://doi:10.1016/j.jenvman.2017.10.002.

Gilbert, J. P., Chelini, M. C., Rosenthal, M. F., Delong, J. P., 2016. Crossing regimes of temperature dependence in animal movement. Global Change Biology. 22(5):1722-1736. https://doi.org/10.1111/gcb.13245.

Gitelson, A., Peng, Y., Huemmrich, K. F., 2014. Relationship between fraction of radiation absorbed by photosynthesizing maize and soybean canopies and NDVI from remotely sensed data taken at close range and from MODIS 250 m resolution data. Remote Sensing of Environment. 147:108-120. https://doi.org/10.1016/j.rse.2014.02.014.

Gomez-Gimenez, M., Jong, R., Peruta, R. D., Keller, A., et al., 2017. Determination of grassland use intensity based on multi-temporal remote sensing data and ecological indicators. Remote Sensing of Environment. 198(C):126-139. https://doi.org/10.1016/j.rse.2017.06.003.

Grace, J. B., Anderson, T. M., Olff, H., Scheiner, S. M., 2010. On the specification of structural equation models for ecological systems. Ecological monographs, 80(1):67-87. https://doi.org/10.1890/09-0464.1.

Grossmann, K, Frankenberg, C, Magney, T. S., et al., 2018. PhotoSpec: A new instrument to measure spatially distributed red and far-red Solar-Induced Chlorophyll Fluorescence, Remote Sensing of Environment, 216:311-327. https://doi.org/10.1016/j.rse.2018.07.002.

Guetté, A. , Godet, L. , Juigner, M. , Robin, M., 2018. Worldwide increase in Artificial Light At Night around protected areas and within biodiversity hotspots. Biological Conservation, 223:97–103. https://.doi.org/10.1016/j.biocon.2018.04.018.

Guha, S., Govil, H., Dey, A., Gill, N., 2018. Analytical study of land surface temperature with NDVI and NDBI using Landsat 8 OLI and TIRS data in Florence and Naples city, Italy. European Journal of Remote Sensing, 51:667-678. https://doi.org/10.1080/22797254.2018.1474494.

Hair, J. F., Black, W. C., Babin, B. J., Anderson, E., Tathan, R. L., 2009. Análise Multivariada de Dados. Porto Alegre: Bookman, 6 ª ed.

Hanks, E. M., Hooten, M. B., and Alldredge, M. W., 2015. Continuous-time discrete-space models for animal movement. Annals of Applied Statistics, 9(1), 145-165. https://doi.org/10.1214/14-AOAS803.

Hoagland, S. J., Beier, P., Lee, D., 2018.Using MODIS NDVI phenoclasses and phenoclusters to characterize wildlife habitat: Mexican spotted owl as a case study. Forest Ecology and Management. 412:80-93. https://doi.org/10.1016/j.foreco.2017.12.017.

Hooten, M. B., Johnson, D. S., Hanks, E. M. and Lowry, J. H. (2010). Agent-based inference for animal movement and selection. J. Agric. Biol. Environ. Stat. 15 523–538. MR2788638

Huang, Q., Yang, X., Gao., B., et al. 2014. Application of DMSP/OLS Nighttime Light Images: A Meta-Analysis and a Systematic Literature Review. Remote Sensing, 6(8):6844-6866. https://doi.org/10.3390/rs6086844.

IBGE – Instituto Brasileiro de Geografia e Estatística. 2012. Mapa de Vegetação do Brasil. Available in https://geoftp.ibge.gov.br/informacoes_ambientais/vegetacao/mapas/brasil/vegetacao.pdf. Accessed on march, 2021.

IBGE – Instituto Brasileiro de Geografia e Estatística. 2021. São Paulo/SP. Available in https://cidades.ibge.gov.br/brasil/sp/sao-paulo/panorama. Accessed on march, 2021.

Ito, T. Y., Sakamoto, S., Lhagvasuren, B., Kinugasa, T., et al., 2018 Winter habitat of Mongolian gazelles in areas of southern Mongolia under new railroad construction: An estimation of interannual changes in suitable habitats. Mammalian Biology, 93:13-20. https://doi.org/10.1016/j.mambio.2018.07.006.

Johnson, H. E., Gustine, D. D., Golden, T. S., Adams, L. G., et al., 2018. NDVI exhibits mixed success in predicting spatiotemporal variation in caribou summer forage quality and quantity. Ecosphere. 9(10):1-19. https://doi.org/10.1002/ecs2.2461.

Kaplan, D., 2000. Structural equation modeling: foundations and extensions. Thousand Oaks: Sage Publications.

Keenleyside, KA; Dudley, N., Cairns, S., Corredor, CM, Stolton, S.,2012. Restauração Ecológica para Unidades de Conservação: Princípios, Diretrizes e Melhores Práticas.União Internacional para a Conservação da Natureza.

König, H. J., Kiffner, C., Kramer-Schadt, S., et al., 2020. Human – wildlife coexistence in a changing world. Conservation Biology. 34(4):786-794. https://doi.org/10.1111/cobi.13513.

Krishnamurthy, R., Cushman, S. A., Sarkar, M. S. et al. 2016. Multi-scale prediction of landscape resistance for tiger dispersal in central India. Landscape Ecology. 31:1355–1368. https://doi.org/10.1007/s10980-016-0363-0.

Krosby, M., Breckheimer, I., John Pierce, D. et al., 2015. Focal species and landscape "naturalness" corridor models offer complementary approaches for connectivity conservation planning. Landscape Ecology. 30: 2121–2132. https://doi.org/10.1007/s10980-015-0235-z.

Kurz, D. J., Nowakowski, A. J., Tingley, M. W., 2014. Forest-land use complementarity modifies community structure of a tropical herpetofauna. Biological Conservation. 170:246-255. https://doi.org/10.1016/j.biocon.2013.12.027.

Levin, N., Zhang, Q., 2017. A global analysis of factors controlling VIIRS nighttime light levels from densely populated areas. Remote Sensing of Environment. 190:366-382. https://doi.org/10.1016/j.rse.2017.01.006.

Lin, B. B., Egerer, M. H., Liere, H., et al., 2018. Local- and landscape-scale land cover affects microclimate and water use in urban gardens. Science of the Total Environment. 610/611:570-575. https://doi.org/10.1016/j.scitotenv.2017.08.091.

Lindenmayer, D. B., Blanchard, W., Foster, C. N., Scheele, B. C. et al., 2020. Habitat amount versus connectivity: an empirical study of bird responses. Biological Conservation. 241:108377. https://doi.org/10.1016/j. biocon.2019.108377.

Liu, C., Newell, G., White, M., Bennett, A. F., 2018. Identifying wildlife corridors for the restoration of regional habitat connectivity: A multispecies approach and comparison of resistance surfaces. PLoS ONE. 13(11), 2018. https://doi.org/10.1371/journal.pone.0206071.

Loveridge, A. J., Valeix, M., Elliot, N. B., et al., 2017. The landscape of anthropogenic mortality: how African lions respond to spatial variation in risk. Journal of Apllied Ecology. 54(3):815-825. https://doi.org/10.1111/1365-2664.12794 .

Luhring, T. M., DeLong, J. P., 2017. Scaling from Metabolism to Population Growth Rate to Understand How Acclimation Temperature Alters Thermal Performance, Integrative and Comparative Biology, 57(1):103–111. https://doi.org/10.1093/icb/icx041.

Marulli, J., Mallarach, J. M., 2005. A GIS methodology for assessing ecological connectivity: application to the Barcelona Metropolitan Area. Landscape and Urban Planning. 71:243-262. https:// doi.org/10.1016/j.landurbplan.2004.03.007.

Mateo-Sánchez, M. C., Balkenhol, N., Cushman, S., et al., 2015. A comparative framework to infer landscape effects on population genetic structure: are habitat suitability models effective in explaining gene flow? Landscape Ecology. 30:1405–1420b. https://doi.org/10.1007/s10980-015-0194-4.

McCann, N. P., Moen, R. A., Windels, S. K., Harris, T.R., 2016 Bed sites as thermal refuges for a cold-adapted ungulate in summer. Wildl Biol. 22:228–237. https://doi.org/10.2981/wlb.00216.

736 Melin, M., et al. 2016. Ecological dimensions of airborne laser scanning - analyzing the role of forest
737 structure in moose habitat use within a year. Remote Sensing of Environment 173:238–247.
738 https://doi.org/10.1016/j.rse.2015.07.025.

739 Milanesi, P., Holderegger, R., Bollmann, K., et al., 2017. Three-dimensional habitat structure and
740 landscape genetics: a step forward in estimating functional connectivity. Ecology. 98(2):393-
741 402. https://doi.org/10.1002/ecy.1645.

742 Mills, E. C., J. R. Poulsen, J. M. Fay, P. Morkel, C. J. Clark, A. Meier, et al. 2018. Forest elephant
743 movement and habitat use in a tropical forest-grassland mosaic in Gabon. PLoS
744 ONE 13:e0199387. https://doi.org/10.1371/journal.pone.0199387.

745 Ministério do Meio Ambiente (MMA), 2021. Áreas prioritárias para conservação da biodiversidade
746 brasileira. http://areasprioritarias.mma.gov.br/1-atualizacao-das-areas-prioritarias /
747 (Accessed on March 8, 2021).

748 Moraes, A. M, Ruiz-Miranda, C. R., Galetti, P. M., et al. 2018. Landscape resistance influences
749 effective dispersal of endangered golden lion tamarins within the Atlantic Forest. Biological
750 Conservation. 224:178-187. https://doi.org/10.1016/j.biocon.2018.05.023.

751 Mörtberg, U., Haas, J., Zetterberg, A. et al., 2013. Urban ecosystems and sustainable urban
752 development—analysing and assessing interacting systems in the Stockholm region. Urban
753 Ecosyst 16:763–782. https://doi.org/10.1007/s11252-012-0270-3.

754 Nandy, S., Singh, R., Ghosh, S. et al., 2017. Neural network-based modelling for forest biomass
755 assessment. Carbon Management. 8(2).
756 http://dx.doi.org/10.1080/17583004.2017.1357402.

757 Nascimento-Júnior, L., 2017. Urbanização e cidade dispersa: implicações da produção do espaço
758 urbano no Brasil, em Moçambique e na Austrália. GEOUSP Espaço E Tempo
759 (Online), 21(2):550-569. https://doi.org/10.11606/issn.2179-0892.geousp.2017.125392.

760 Neumann, J.E., Price, J., Chinowsky, P. et al., 2015. Climate change risks to US infrastructure:
761 impacts on roads, bridges, coastal development, and urban drainage. Climatic
762 Change 131:97–109. https://doi.org/10.1007/s10584-013-1037-4

763 Nimmo, D.G., Mac Nally, R., Cunningham, S.C., Haslem, A., Bennett, A. F., 2015. Vive la
764 résistance: reviving resistance for 21st century conservation, Trends in Ecology & Evolution.
765 30(9):516-523. https://doi.org/10.1016/j.tree.2015.07.008.

766 Niu, X., Tang, J., Wang, S., et al. 2019. Impact of future land use and land cover change on
767 temperature projections over East Asia. Clim Dyn 52:6475–6490.
768 https://doi.org/10.1007/s00382-018-4525-4

769 Nowakowski, A. J., Wating, J. L., Whitfield, S. M., et al., 2016. Tropical amphibians in shifting
770 thermal landscapes under land-use and climate change. Conservation Biology. 31(1):96-
771 105. https://doi.org/10.1111/cobi.12769.

772 Ojima, R. 2007. Dimensões da urbanização dispersa e proposta metodológica para estudos
773 comparativos: uma abordagem socioespacial em aglomerações urbanas brasileiras. R.
774 Brasileira de Estudos de População. 24(2):277-300. https://doi.org/10.1590/S0102-
775 30982007000200007.

776 Osmond, M.M., Barbour, M.A., Bernhardt, J.R, Pennell, M.W., Sunday, et al.,2017. Warming-
777 induced changes to body size stabilize consumer-resource dynamics. American
778 Naturalist. 189(6):718-725. https://doi.org/ 10.1086 / 691387.

779 Pawar, S., Dell, A. I., Savage, V. M., Knies, J. L. 2016. Real versus artificial variation in the thermal
780 sensitivity of biological traits. American Naturalist. 187:E41–
781 E52. https://doi.org/10.1086/684590.

782 Peterman, W. E., Connette, G. M., Semlitsch, R. D., Eggert, L. S., 2014. Ecological resistance
783 surfaces predict fine-scale genetic differentiation in a terrestrial woodland salamander.
784 Molecular Ecology. 23:2402–2413. https://doi.org/10.1111/mec.12747.

785 Pettorelli, N., Owen, H. J. F., Ducan, C., 2016. How do we want Satellite Remote Sennsing to
786 support biodiversity conservation globally? Methods in Ecology and Evolution. 7(6):656-665.
787 https://doi.org/10.1111/2041-210X.12545.

788 Pettorelli, N., Ryan, S. J., Mueller, T., et al., 2011. The Normalized Difference Vegetation Index
789 (NDVI): Unforeseen successes in animal ecology. Climate Reaserch. 46:15-27.
790 https://doi.org/ 10.3354/cr00936.

791 Poniatowski, D., Loffler, F., Stuhldreher, et al., 2016. Functional connectivity as an indicator for
792 patch occupancy in grassland specialists. Ecological Indicator. 67:735–742.
793 https://doi.org/10.1016/j. ecolind.2016.03.047.

794 Reding, D. M., Cushman, S., Gosselink, T. E., Clark, W. R., 2013. Linking movement behavior and
795 fin-scale genetic structure to model landscape connectivity for bobcats (Lynx rufus).
796 Landscape Ecology. 28:471–486. https://doi.org/10.1007/s10980-012-9844-y

797 Remelgado, R., Safi, K., Wegmann, M., 2020. From ecology to remote sensing: using animals to
798 map land cover. 6(1):93-104. https://doi.org/10.1002/rse2.126.

799 Remelgado, R., Safi, K., Wegmann, M., 2020. From ecology to remote sensing: using animald to
800 map land cover. Remote Sensing in Ecology and Conservation. 6(1):93-104.
801 https://doi.org/10.1002/rse2.126.

802 Remelgado, R., B. Leutner, K. Safi, R. Sonnenschein, C. Kuebert, and M. Wegmann. 2018. Linking
803 animal movement and remote sensing – mapping resource suitability from a remote sensing
804 perspective. Remote Sensing in Ecology and Conservation 4:211–
805 244. https://doi.org/10.1002/rse2.70

806 Rickbeil, G. J. M., T. Hermosilla, N. C. Coops, J. C. White, and M. A. Wulder. 2017. Barren-ground
807 caribou (Rangifer tarandus groenlandicus) behaviour after recent fire events; integrating
808 caribou telemetry data with Landsat fire detection techniques. Glob. Change Biol. 23:1036–
809 1047. https://doi.org/10.1111/gcb.13456.

810 Rigden, A. J., Li, D., 2017. Attribution of surface temperature anomalies induced by land use and
811 land cover changes: Attribution of temperature anomalies. 44(13): 6814-6822.
812 https://doi.org/10.1002/2017GL073811.

813 Robinson, N. M., Leonard, S. W. J., Ritchie, E. G., et al., 2013. Review: Refuges for fauna in fire-
814 prone landscapes: their ecological function and importance. Journal of Applied Ecology.
815 50(6):1321-1329. https://doi.org/10.1111/1365-2664.12153.

816 Rousta, I., Sarif, M. O., Gupta, R. D., Olafsson, H., et al., 2018. Spatiotemporal Analysis of Land
817 Use/Land Cover and Its Effects on Surface Urban Heat Island Using Landsat Data: A Case
818 Study of Metropolitan City Tehran (1988–2018). Sustainability. 10(12):1-26.
819 https://doi.org/10.3390/su10124433.

820 Rudnick, D., Beier, P., Cushman, S., et al., 2012. The Role of Landscape Connectivity in Planning
821 and Implementing Conservation and Restoration Priorities. Issues in Ecology. Report No.
822 16. Ecological Society of America. Washington, DC.

823 Salami, B., Higuchi, P. L., Silva, A. C., et al., 2014. Influência de variáveis ambientais na dinâmica
824 do componente arbóreo em um fragmento de Floresta Ombrófila Mista em Lages, SC.
825 Scientia Forestalis, Piracicaba, 42(102):197-207. https://doi.org/10.5902/198050985081.

826 Salgueiro, P. A., Valerio, F., Silva, C., et al., 2021. Multispecies landscape functional connectivity
827 enhances local bird species' diversity in a highly fragmented landscape. Journal of
828 Environmental Management. 284:112066. https://doi.org/10.1016/j.jenvman.2021.112066

Salt, J. L., Bulit, C., Zhang, W., Qi, H., Montagnes, D. J. S., 2017. Spatial extinction or persistence: landscape-temperature interactions perturb predator–prey dynamics. Ecography. 40(10):1177-1186. https://doi.org/ 10.1111 / ecog.02378.

Santos, A. R, Oliveira, F. S., Silva, A. G., et al. 2017. Spatial and temporal distribution of urban heat islands. Science of the Total Environmental. 605/606:946–956. https://doi.org/10.1016/j.scitotenv.2017.05.275.

Sawyer, S. C., Epps, C. W., Brashares, J. S. 2011. Placing linkages among fragmented habitats: do least-cost models reflect how animals use landscapes? Journal Appl. Ecology. 48:668–678. https://doi.org/10.1111/j.1365-2664.2011.01970.x.

Shen, M., Piao, S., Chen, X., et al., 2016. Strong impacts of daily minimum temperature on the green-up date and summer greenness of the Tibetan Plateau. Global Change Biology. 22(9):3057-3066. https://doi.org/10.1111/gcb.13301.

Shi, Y., Huang, W., Dong, Y., Peng, D., et al., 2018. The influence of landscape's dynamics on the Oriental Migratory Locust habitat change based on the time-series satellite data. Journal of Environmental Management. 218:280-290. https://doi.org/10.1016/j.jenvman.2018.04.028.

Silva, J. S., Silva, R. M., Santos, C. A. G., 2018. Spatiotemporal impact of land use/land cover changes on urban heat islands: A case study of Paço do Lumiar, Brazil. Building and Environment. 136:279-292. https://doi.org/10.1016/j.buildenv.2018.03.041.

Smith, M. J., Goodchild, M. F., Longley, P. A, et al., 2018. Geospatial Analysis. A comprehensive guide to principles techniques and software tools. 6º ed. Available in https://www.spatialanalysisonline.com/extractv6.pdf. Accessed in May 2020.

Spear, S. F., Storfer, A., 2010. Anthropogenic and natural disturbance lead to differing patterns of gene flow in the Rocky Mountain tailed frog, Ascaphus montanus. Biological Conservation. 143(3):778-786. https://doi.org/10.1016/j.biocon.2009.12.021.

Su, Y., Chen, X., Wang, C., Zhang, H., et al., 2015 A new method for extracting built-up urban areas using DMSP-OLS nighttime stable lights: a case study in the Pearl River Delta, southern China, GIScience & Remote Sensing, 52(2):218-238, https://doi.org/10.1080/15481603.2015.1007778.

Sunday, J. M., Bates, A.E., Kearney, M. R., et al. 2014. Thermal-safety margins and the necessity of thermoregulatory behavior across latitude and elevation. Proc Natl Acad Sci USA 201316145. https://doi.org/10.1073/pnas.1316145111.

Theobald D. M., Reed S. E., Fields K., Soulé M. 2012. Connecting natural landscapes using a landscape perme-ability model to prioritize conservation activities in the United States. Conserv Lett. 5:123–133. https://doi.org/10.1111/j.1755-263X.2011.00218.x.

Ullman, J. B., 2006. Structural equation modeling. In Tabachnick, B.G.& Fidell, L.S. (Eds.), Using multivariate statistics (653-771). Boston: Ally & Bacon.

Union Nations Educations, Scientific and Cultural Organization (UNESCO), 2019. Biosphere Reserves. https://en.unesco.org/biosphere / (Accessed on November 20, 2019).

USGS. 2019. Landsat Missions: Using the USGS Landsat8 Product. U.S. Department of the Interior - U.S. Geological Survey. Available in https://www.usgs.gov/land-resources/nli/landsat/using-usgs-landsat-level-1-data-product. Accessed in September 2019.

Wasserman, T. N., Cushman, S. A., Schwartz, M. K. et al. 2010. Spatial scaling and multi-model inference in landscape genetics: Martes americana in northern Idaho. Landscape Ecology. 25:1601–1612. https://doi.org/10.1007/s10980-010-9525-7.

Weber, D., Schaepman-Strub, G., Ecker, K., 2018. Predicting habitat quality of protected dry grasslands using Landsat NDVI phenology. Ecological Indicators 91:447-460. https://doi.org/10.1016/j.ecolind.2018.03.081.

Wei, B., Xie., Y., Jia, X., et al., 2018. Land use/land cover change and it's impacts on diurnal temperature range over the agricultural pastoral ecotone of Northern China. Land Degradation & Development. 29(9):3009–3020. https://doi.org/10.1002/ldr.3052.

Wilson, K., Hanks, E. M, and Johnson, D., 2019. Estimating animal utilization densities using continuous-time Markov chain models. Methods in Ecology and Evolution. 9(5):1232-1240. https://doi.org/10.1111/2041-210X.12967.

Woodley, S, J. 2010. Integridade ecológica e parques nacionais do Canadá. Fórum George Wright. 27:151-160.

Zeller, K.A., McGarigal, K., Whiteley, A. R., 2012. Estimating landscape resistance to movement: a review. Landscape Ecology. 27(6):777–797. https://doi.org/10.1007 / s10980-012-9737-0.

Zhang, L., Peng, J., Liu, Y. et al. 2017. Coupling ecosystem services supply and human ecological demand to identify landscape ecological security pattern: A case study in Beijing–Tianjin–Hebei region, China. Urban Ecosyst 20:701–714. https://doi.org/10.1007/s11252-016-0629-y.

891 Zhou, X., Chen, H., 2018. Impact of urbanization-related land use land cover changes and urban
892 morphology changes on the urban heat island phenomenon. Science of the Total
893 Environmental. 635:1467-1476. https://doi.org/10.1016/j.scitotenv.2018.04.091.

Figures

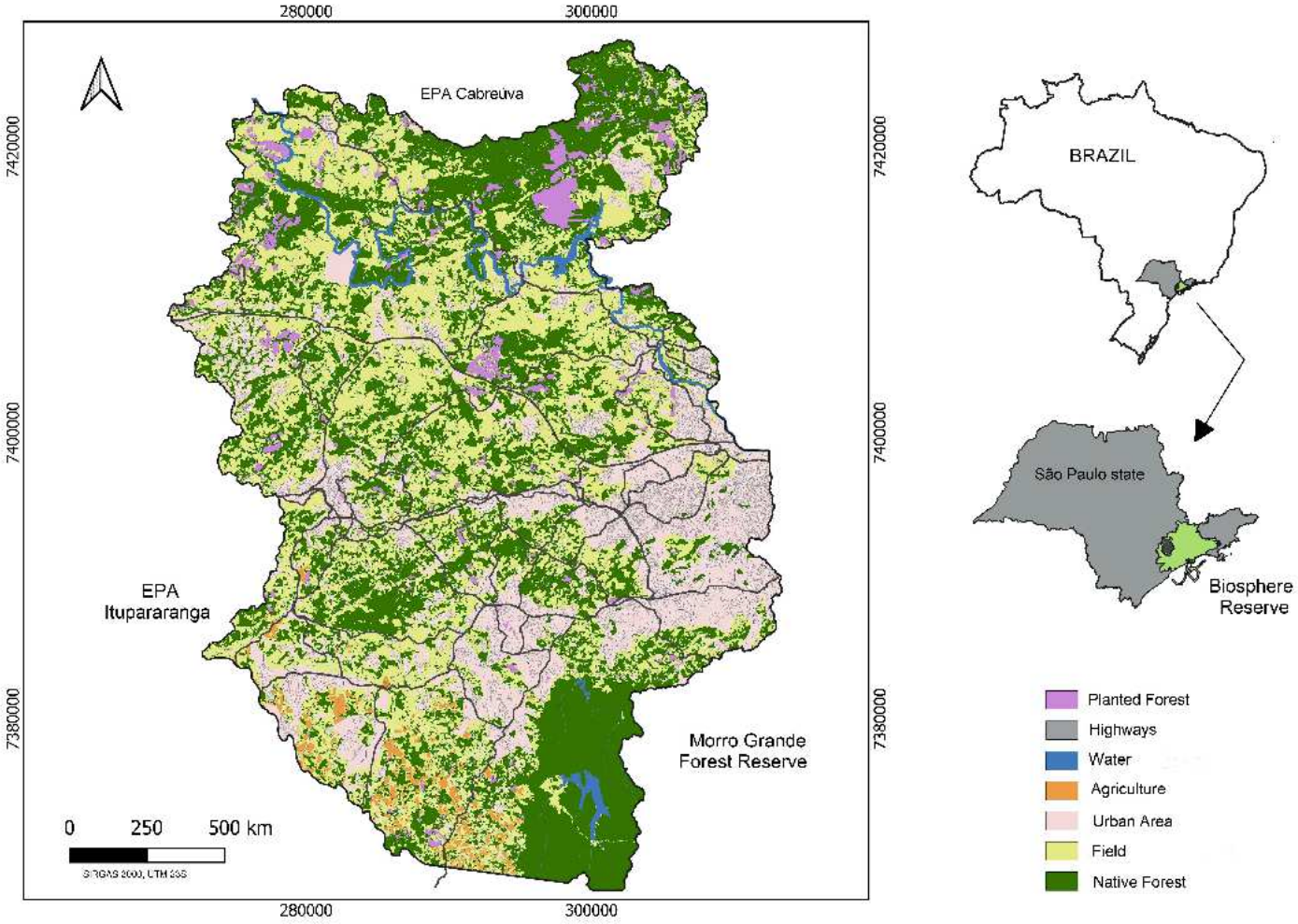

Figure 1

Land Use/Land Cover (LULC) and location of the study Landscape in the Green Belt Biosphere Reserve of São Paulo City (GBBR-SP), Brazil. Note: The designations employed and the presentation of the material on this map do not imply the expression of any opinion whatsoever on the part of Research Square concerning the legal status of any country, territory, city or area o bbnhjr of its authorities, or concerning the delimitation of its frontiers or boundaries. This map has been provided by the authors.

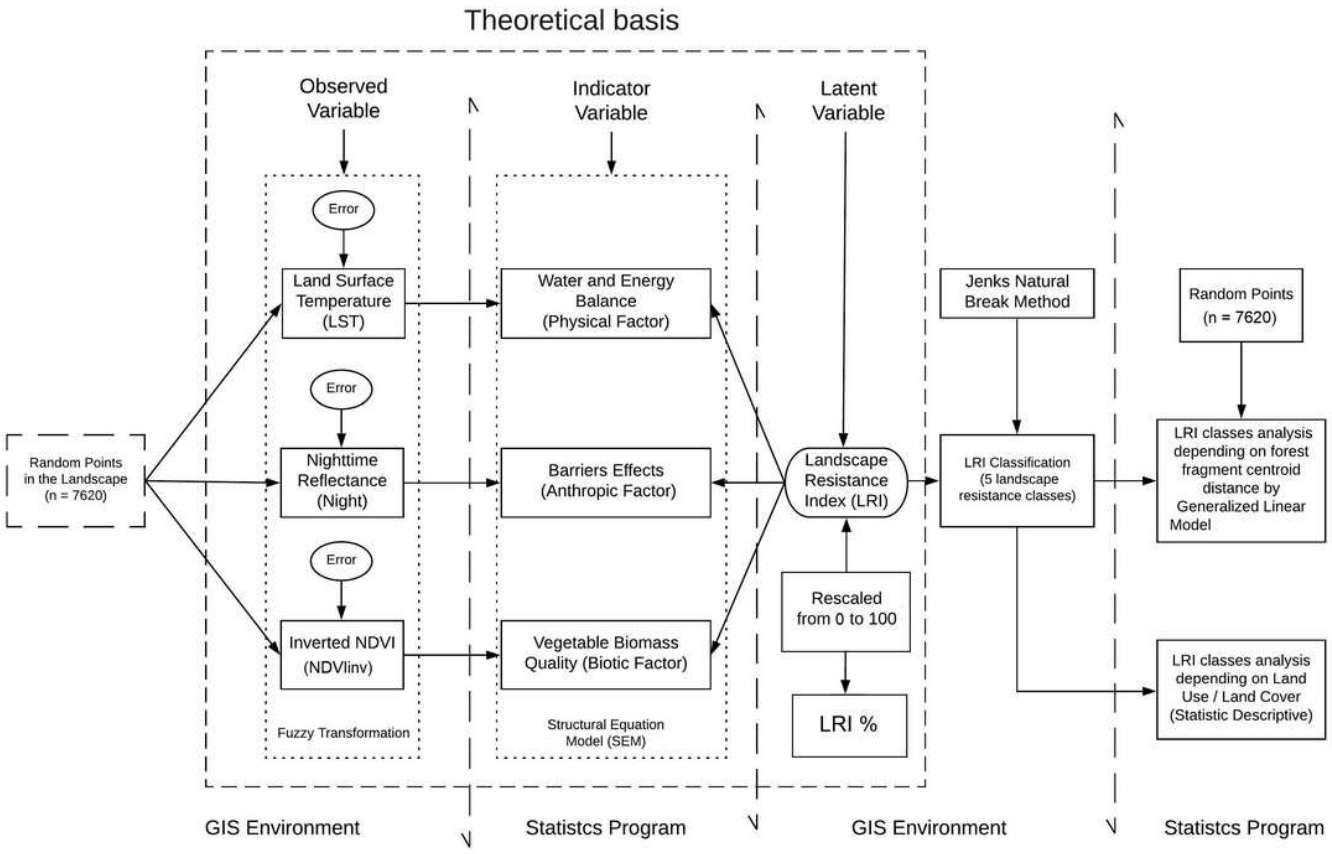

Figure 2

Conceptual model used to obtain the Landscape Resistance Index for the Green Belt Biosphere Reserve of São Paulo City (GBBR-SP), Brazil.

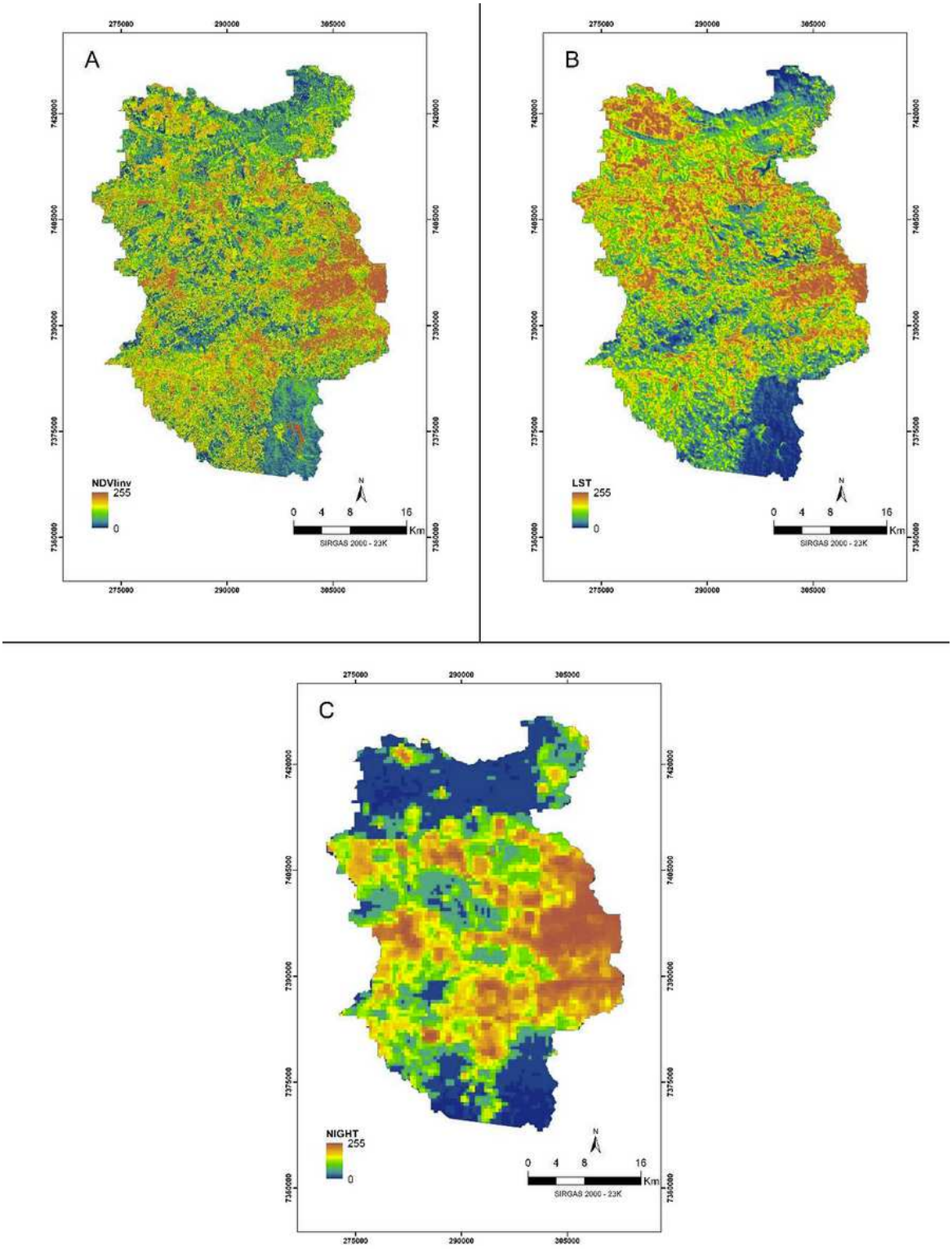

Figure 3

Environmental attributes (in 255 bytes) for the study area in the GBBR-SP, Brazil: (A) Inverted NDVI, (B) Land Surface Temperature, and (C) Nighttime Reflectance. Note: The designations employed and the presentation of the material on this map do not imply the expression of any opinion whatsoever on the part of Research Square concerning the legal status of any country, territory, city or area o bbnhjr of its

authorities, or concerning the delimitation of its frontiers or boundaries. This map has been provided by the authors.

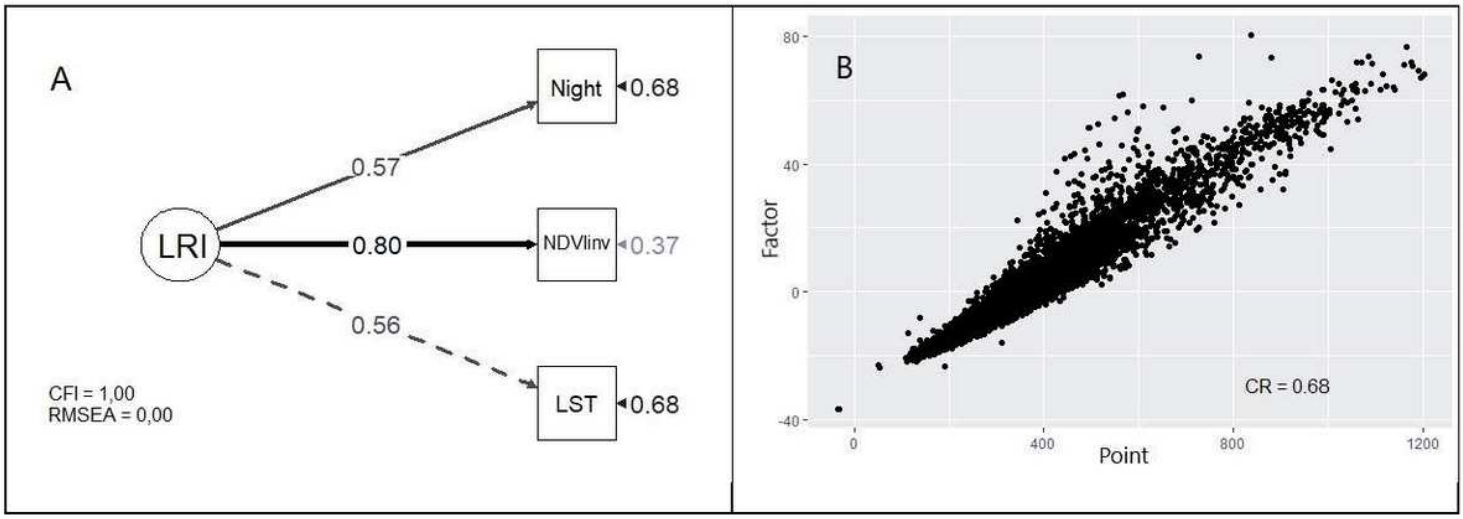

Figure 4

Landscape Resistance Index for the study area in the GBBR-SP, Brazil: (A) parameters and factor loadings modeled, and (B) model CR, based on the sum of the points representing the OV and their factor loadings.

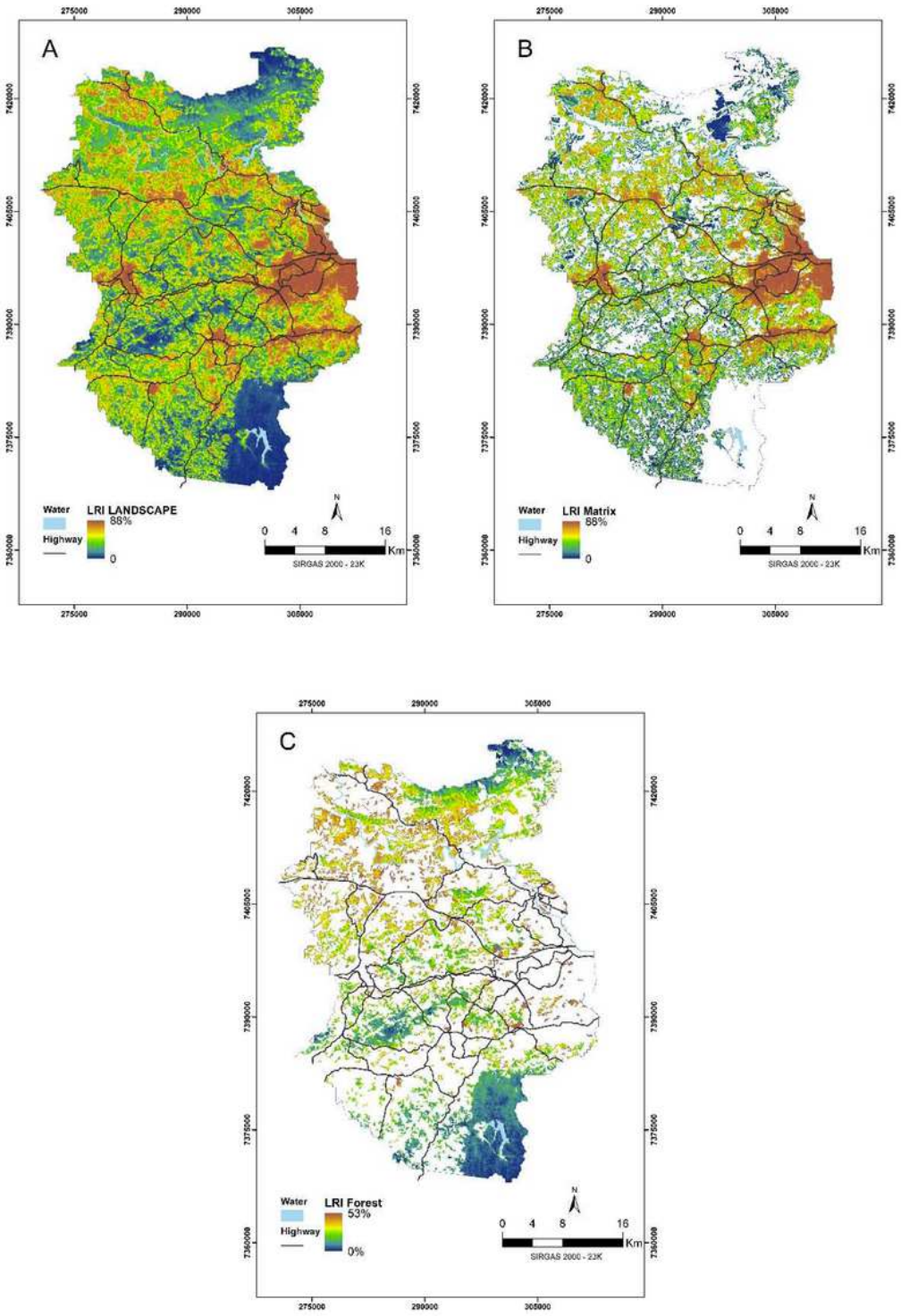

Figure 5

LRI% spatialized through the studied area (Fig. 5A), without the forest patches (Fig. 5B), and only inside these patches (Fig. 5C). Note: The designations employed and the presentation of the material on this map do not imply the expression of any opinion whatsoever on the part of Research Square concerning the legal status of any country, territory, city or area o bbnhjr of its authorities, or concerning the delimitation of its frontiers or boundaries. This map has been provided by the authors.

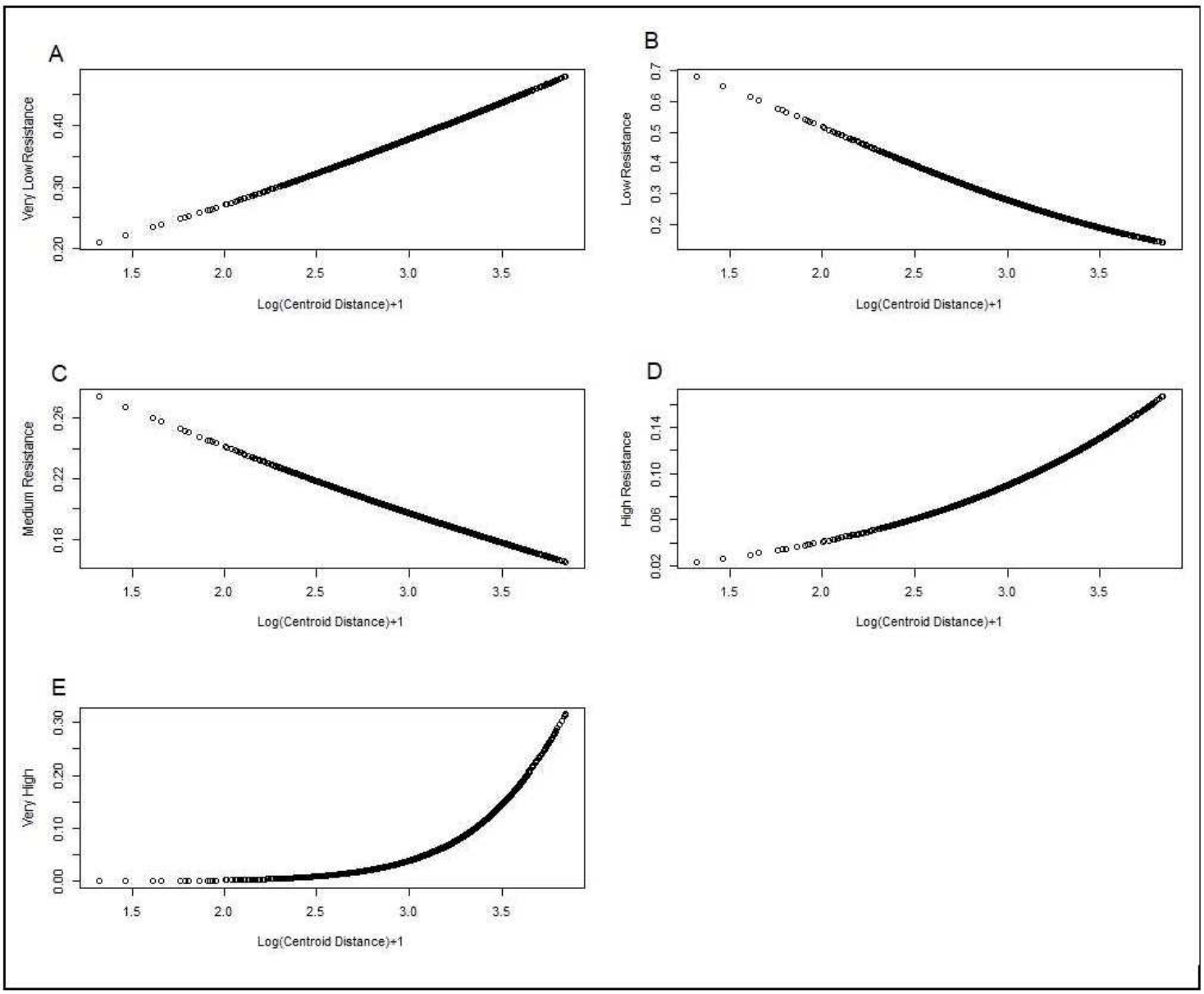

Figure 6

Binomial regression Generalized Linear Model (GLM) for LRI resistance classes, depending on forest patches distance from their centroids of the studied landscape, in the GBBR-SP, Brazil.

Supplementary Files

This is a list of supplementary files associated with this preprint. Click to download.

- Table.pdf